Understanding the geometrical properties of an Ames room and controlling it systematically and quantitatively

Vladislav Myrov, Elena Gorina, Kristina Vodorezova, Maria Dvoeglazova, Ekaterina Koshmanova, Elena S. Gorbunova, Tadamasa Sawada

Abstract

Within an Ames room, the perceived size of objects, such as people, changes dynamically when the objects move about within the room. The shape of the Ames room is not actually rectangular but it is perceived to be rectangular. Unfortunately, the geometrical properties of the Ames room have often been misunderstood, and rooms that have different shapes are also referred to as “Ames rooms” in many articles. In this study, the geometrical properties of the original Ames rooms constructed by Adelbert Ames, Jr. were analyzed and the generalization of the Ames room was discussed. We found that these original Ames rooms are 3D-to-3D perspective transformations of rectangular illusory rooms. Based on this analysis, we also developed a computational model that can construct a generalized Ames room that has a hexahedral shape with some free parameters that quantitatively control (i) the size and aspect-ratio of a rectangular illusory room, (ii) the amount of distortion of the Ames room from a rectangular room, and (iii) the viewpoint of an observer. This model was implemented as a computational program so that an Ames room can be constructed in a VR space. Note that the transformations of the Ames rooms can be applied to an arbitrary 3D scene and that they can be regarded as members of a subset of 3D-to-3D perspective transformations. Any perspective transformation in this subset distorts the 3D scene in such a way that the retinal image of the distorted scene, when seen from a specific viewpoint, is identical to the retinal image of the initial scene, when seen from a specific viewpoint. These generalizations allow us to control the conditions of an Ames room systematically with more flexibility when we study this illusion.

Understanding the geometrical properties of an Ames room and controlling it systematically and quantitatively

Vladislav Myrov[1], Elena Gorina[2], Kristina Vodorezova[2], Maria Dvoeglazova[2], Ekaterina Koshmanova[3], Elena S. Gorbunova[2], Tadamasa Sawada[2,4,5,6*]

[1]Department of Neuroscience and Biomedical Engineering, Aalto University, Espoo, 02150, Finland

[2]School of Psychology, HSE University, Moscow, 101000, Russia

[3]GIGA - Cyclotron Research Centre In Vivo Imaging, University of Liège, Liège, 4000, Belgium

[4]Akian College of Science and Engineering, American University of Armenia, Yerevan, 0019, Armenia

[5]Department of Psychology, Russian-Armenian (Slavonic) University, Yerevan, 0051, Armenia

[6]European University of Armenia, Yerevan, 0037, Armenia

*tada.masa.sawada@gmail.com

Abstract

Within an Ames room, the perceived size of objects, such as people, changes dynamically when the objects move about within the room. The shape of the Ames room is not actually rectangular but it is perceived to be rectangular. Unfortunately, the geometrical properties of the Ames room have often been misunderstood, and rooms that have different shapes are also referred to as “Ames rooms” in many articles. In this study, the geometrical properties of the original Ames rooms constructed by Adelbert Ames, Jr. were analyzed and the generalization of the Ames room was discussed. We found that these original Ames rooms are 3D-to-3D perspective transformations of rectangular illusory rooms. Based on this analysis, we also developed a computational model that can construct a generalized Ames room that has a hexahedral shape with some free parameters that quantitatively control (i) the size and aspect-ratio of a rectangular illusory room, (ii) the amount of distortion of the Ames room from a rectangular room, and (iii) the viewpoint of an observer. This model was implemented as a computational program so that an Ames room can be constructed in a VR space. Note that the transformations of the Ames rooms can be applied to an arbitrary 3D scene and that they can be regarded as members of a subset of 3D-to-3D perspective transformations. Any perspective transformation in this subset distorts the 3D scene in such a way that the retinal image of the distorted scene, when seen from a specific viewpoint, is identical to the retinal image of the initial scene, when seen from a specific viewpoint. These generalizations allow us to control the conditions of an Ames room systematically with more flexibility when we study this illusion.

Introduction

An Ames room is the interior space of a non-rectangular hexahedron that is designed in such a way that the retinal image of the room, when seen from a specific viewpoint, becomes identical to the retinal image of a rectangular room when seen from a specific view point. The room is perceived to be rectangular and the perceived size of objects within the room, such as human beings, changes dynamically when the objects move about within the room (Day, 1993; Ittelson, 1952, see

https://youtu.be/W_5wpPxCcyw?t=1254). This illusion is vivid and an Ames room is often physically constructed in many science museums.

Adelbert Ames Jr. (Behrens, 1987) constructed a few different types of such a distorted room but the Ames room usually refers to a "monocular distorted room no. 1" or a "full size monocular distorted room" in Ittelson (1952, pp. 39–45; Ittelson & Ames, 1968). Unfortunately, the geometrical properties of these Ames room have often been misunderstood, and rooms that have different shapes are also referred to as "Ames rooms" in many articles (Koshmanova et al., in-press). For clarity, these different "Ames rooms" are referred to as sundry-Ames rooms in this article. Some of the sundry-Ames rooms (Brecher & Puno, 2010; Wang et al., 2022; Williford, et al., 2022; Goldstein, 2007; Rossing & Chiaverina, 2019; Wickelgren, 2012, see also Rogers, 2022; Tyler, 2022; Gogel & Mershon, 1968) can still be projected to a retinal image that is identical to the retinal image of the rectangular illusory room but they have floors and ceilings that are non-planar and their identical retinal image is more accidental than the identical retinal image of the original Ames room (see Koshmanova et al., in-press). There is also a sundry-Ames room whose retinal image cannot be identical to the retinal image of an illusory rectangular room (JoVE, 2023; Stewart, 1974, see also Gregory, 1966).

These accidentalness and non-identicalness of the retinal images of the sundry-Ames rooms could act as artifacts in studies of the Ames room illusion. Stewart (1974) conducted a cross-cultural study to test the Ames room illusion and the result of the study was different from both predicted trends based on the empiricism and on the nativism.[1] Note that Stewart (1974, Fig. 1) used the sundry-Ames room whose retinal image cannot be identical to the retinal image of an illusory rectangular room. The sensitivity to the difference of the retinal image may explain the insusceptibility to the Ames room illusion. Gibson (1979, p. 168) argued that the Ames room illusion diminishes after seeing the distorted room binocularly from various viewpoints while Ittelson (1960, p.149) reported the illusion recovers even after seeing the room binocularly when the room is seen monocularly (see also Runeson, 1988). This difference between these studies may be explained if Gibson (1979) used a sundry-Ames room. An observer may find visual cues that indicate the distortion of the sundry-Ames room, like shading of the non-planar floor or the inconsistency of its retinal image to an illusory rectangular room.

It is critical to systematically control the distal and proximal stimuli in a psychophysical experiment that is testing the visual perception. In the study of the 3D perception, the distal stimulus is a 3D scene and the proximal stimulus is the 2D projection of the 3D scene. It is not a trivial task to design and to control the visual stimuli for studying a specific aspect of the 3D perception without introducing any artifacts (see Li et al., 2012; Minkov & Sawada, 2021; Mischenko et al., 2020; Pizlo & Salach-Golyska, 1994; Sawada & Dvoeglazova, 2023; Sawada & Pizlo, 2022). Note also that recovering the 3D information from the 2D projection is an ill-posed inverse problem. This problem is under-constrained and there are infinitely many 3D interpretations that could have produced the same 2D image. Despite this fact, the visual system often recovers a *unique* 3D interpretation (Pizlo et al., 2014). Understanding the geometrical properties of the 3D information and its 2D projection is required to control the visual stimuli and to discuss the results of the experiment to infer how the visual system is recovering the 3D information.

There are multiple potential factors that can produce the Ames room illusion, such as the rectangularity (Dvoeglazova & Sawada, 2024) and the symmetry (Pizlo et al., 2014) of the shape of the illusory room as well as the parallelism of the line-segments (Dvoeglazova et al., 2021), the horizontalness of

[1] There are some other concerns with Stewart (1974) using the current methodological standard (see also Dvoeglazova & Sawada, 2024, pp. 11-12 for a relevant discussion). For example, it seems that Stewart (1974) made an additional prediction after observing the result to conclude that the Ames room illusion is empirical but this can be regarded as HARKing (Kerr, 1998; Simmons et al., 2011).

the floor, and the textures of the walls and the floor in the illusory room. Systematic control of these factors is required to study the factors and analytical understanding of the factors is required to control them (see Sugihara, 1986, 1997, 2005, 2014a, 2014b; Cowan, 1974, 1977a, 1977b, 1982; Sawada & Dvoeglazova, 2023; Sawada & Volk, 2024; Sawada et al., 2011, 2014 for analytical discussions of some other 3D geometrical illusions).

In this study, we analyze the geometrical properties of an Ames room (the "monocular distorted room no. 1," Ittelson, 1952) and show that the Ames room is a 3D-to-3D projective transformation of a rectangular illusory room. This transformation is generalized to a subset of 3D-to-3D projective transformations so that an arbitrary rectangular room (the section "A generalized Ames room") and an arbitrary 3D scene (the section "An Ames scene") can be distorted without changing their 2D retinal images from their specific viewpoints. The planarity of faces and the straightness of line-segments in the rectangular room and in the scene are invariants of this distortion. Based on this analysis, we also develop a computational model that can construct a generalized Ames room of a hexahedral shape with some free parameters that quantitatively control (i) the size and aspect-ratio of a rectangular illusory room, (ii) the amount of distortion of the Ames room from a rectangular room, and (iii) the viewpoint of an observer. The model is also implemented as a computational program (https://github.com/TadamasaSawada/AmesRoom, https://youtu.be/CfF_rLsPEt8).

Analysis

Monocular distorted room no. 1

First, the relationship between the "monocular distorted room no. 1" in Ittelson (1952, pp. 39–43) and its rectangular illusory room is considered. This distorted room is referred to as the *original Ames room* in this study.

The 3D XYZ Cartesian coordinate system is set to a 3D scene based on the rectangular illusory room in the scene. The rectangular room is cubic and its six faces are planar squares. A viewpoint of the rectangular room is at the center of one of its walls. An observer sees the interior of the room from this point. This wall is referred to as the *viewing wall* in this study. The wall that is on the other side of the rectangular room and that is facing to the observer is referred to as the *facing wall*. The four walls are vertical and the floor and the ceiling are horizontal in the rectangular room. The coordinate system is left-handed. The origin of the coordinate system is at the viewpoint. The Y-axis is vertical and it is upward. The X- and Z-axes are horizontal and perpendicular to one another. The X-axis goes from left to right and the Z-axis goes from back to front of an observer at the viewpoint. The XY-plane is coplanar to the viewing wall. The left and right walls of the rectangular rooms are normal to the X-axis, the viewing and facing walls are normal to the Z-axis, and the floor and ceiling are normal to the Y-axis.

The shape and size of the rectangular illusory room and its viewpoint are specified as follows. The width, height, and depth of the rectangular room are 108.36 cm (42.66 in). The four vertices V_{LGF}, V_{LGH}, V_{LCH}, and V_{LCF} of the left wall of the rectangular room are written as:

$$[V_{LGF} \quad V_{LGH} \quad V_{LCH} \quad V_{LCF}] = \begin{bmatrix} -w_L & -w_L & -w_L & -w_L \\ -h_D & -h_D & h_U & h_U \\ d_F & -d_H & -d_H & d_F \end{bmatrix} \tag{1}$$

and the four vertices V_{RGF}, V_{RGB}, V_{RCB}, and V_{RCF} of the right wall of the rectangular room are written as:

$$[V_{RGF} \quad V_{RGH} \quad V_{RCH} \quad V_{RCF}] = \begin{bmatrix} w_R & w_R & w_R & w_R \\ -h_D & -h_D & h_U & h_U \\ d_F & -d_H & -d_H & d_F \end{bmatrix} \tag{2}$$

where $w_L = w_R = h_D = h_U = 54.18$ cm (21.33 in), $d_H = 0$ cm, and $d_F = 108.36$ cm (42.66 in). Note that $w_L+w_R = h_D+h_U = d_F+d_H = 108.36$ cm (42.66 in).

Now, consider constructing the original Ames room based on its information in Ittelson (1952; Ittelson & Ames, 1968) and discussing the mathematical relationship from the rectangular illusory room to the Ames room. The four walls and the floor of the Ames room are planar and their shapes and sizes are specified in Ittelson (1952, pp. 39–43, Figure 1). The Ames room should be constructed from these faces so that its retinal image, when seen from the viewpoint at the origin, becomes identical to the retinal image of the rectangular room. The retinal images of these rooms are 3D-to-2D perspective transformations of the rooms.

Figure 1. The floor, and the four walls of the original Ames room (Ittelson, 1952, pp. 39–43). The floor is a scalene-trapezoid. The left and right walls are squares. The left wall is twice as big as the right wall. The facing and viewing walls are two isosceles-trapezoids. The viewing wall has a hole (black dot) that serves as a viewing position of the Ames room. The shape of the ceiling is not specified in Ittelson (1952). Textures are added to the faces for clarity.

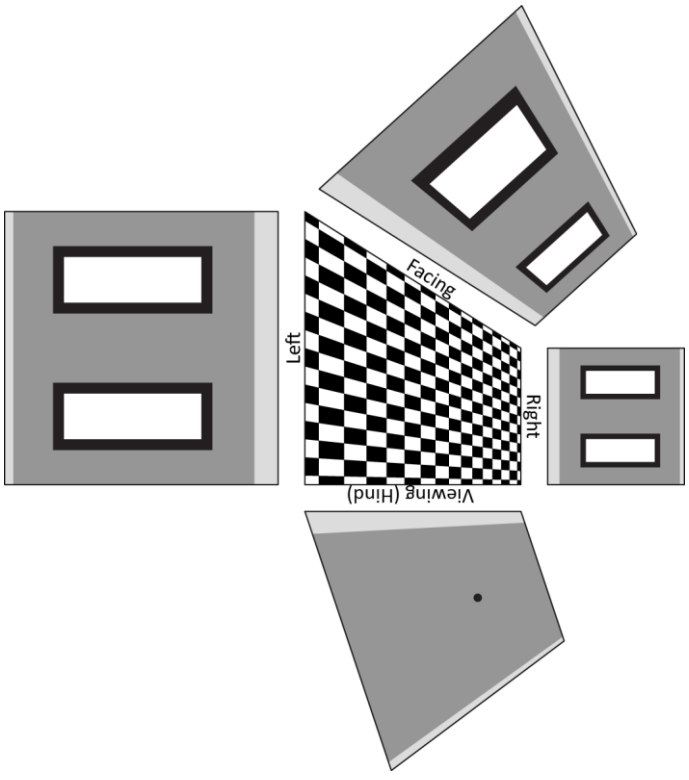

Each of the four walls have a pair of line-segments that correspond to vertical line-segments in the rectangular illusory room. This pair of line-segments of the wall are parallel to one another, so, when the

four walls are composed to form the Ames room, the pairs of parallel line-segments of the individual walls become parallel across the walls. The retinal images of these parallel line-segments of the Ames room coincide with the retinal images of the vertical line-segments of the rectangular room only if these line-segments of the two rooms are parallel across the rooms. If they are, the parallel line-segments of the Ames room are also vertical. This means that all of the four walls of the Ames room are vertical.

The left and right walls of the original Ames room are squares as well as the left and right walls of the rectangular illusory room. The sizes of the left and right walls of the rectangular room are identical to one another and the sizes of the left and right walls of the Ames rooms are 1.5 and 0.75 times the identical size of the left and right walls of the rectangular room. Each of the left and right walls has a pair of vertical line-segments. The other pair of line-segments of the wall are parallel to one another and horizontal. The retinal images of these parallel line-segments should coincide with the retinal images of two line-segments of the rectangular room that are parallel to the Z-axis. If they do, the horizontal line-segments of the left and right walls of the Ames room are also parallel to the Z-axis. This means that the left and right walls of the Ames room are normal to the X-axis and that they are parallel to one another and to the left and right walls of the rectangular room.

The ceiling is composed of two horizontal line-segments from the left and right walls that are parallel to one another and two line-segments from the facing and viewing walls whose lengths are different from one another. This means that the ceiling is also planar and that it is a scalene-trapezoid. This shape is the same as the shape of the floor (Figure 1).

The viewing wall of the original Ames room has a hole, which serves as the viewpoint of the Ames room. The viewing walls of the Ames room and of the rectangular room are coplanar to one another so that their retinal images coincide with one another.

Figure 2 shows the orthographic images of the Ames room and of the rectangular illusory room from the front, side, and top views. Their images of each view are superimposed to one another so that their viewpoints coincide to one another and that the line-of-sight from the viewpoint to each vertex of the rectangular room coincides with the line-of-sight to its corresponding vertex of the Ames room. In each view of Figure 2, the images of the left walls of the Ames room and the rectangular rooms are line-segments that are parallel to one another. These parallel line-segments and the lines-of-sights to the vertices of the left walls form two triangles that are geometrically-similar and are superimposed on one another. Note that the size of the left wall of the Ames room is 1.5 times the size of the left wall of the rectangular room. So, the distance of the left wall of the Ames room from the viewpoint is 1.5 times larger than the distance of the left wall of the rectangular room. In a similar way, the distance of the right wall of the Ames room is 0.75 times the distance of the left wall of the rectangular room. Namely, the four vertices of the left wall of the Ames room can be represented as scaling transformations of V_{LGF}, V_{LGH}, V_{LCH}, and V_{LCF} by a factor of $s_L = 1.5$:

$$[V'_{LGF} \quad V'_{LGH} \quad V'_{LCH} \quad V'_{LCF}] = s_L \begin{bmatrix} -w_L & -w_L & -w_L & -w_L \\ -h_D & -h_D & h_U & h_U \\ d_F & -d_H & -d_H & d_F \end{bmatrix} \tag{3}$$

and the four vertices of the right wall of the Ames room can be represented as scaling transformations of V_{RGF}, V_{RGH}, V_{RCH}, and V_{RCF} by a factor of $s_R = 0.75$:

$$[V'_{RGF} \quad V'_{RGH} \quad V'_{RCH} \quad V'_{RCF}] = s_R \begin{bmatrix} w_R & w_R & w_R & w_R \\ -h_D & -h_D & h_U & h_U \\ d_F & -d_H & -d_H & d_F \end{bmatrix}$$

(4)

where V'_{LGF}, V'_{LGH}, V'_{LCH}, V'_{LCF}, V'_{RGF}, V'_{RGH}, V'_{RCH}, and V'_{RCF} are the vertices of the Ames room. The left and right walls of the Ames room are normal to the X-axis and the walls are connected by four straight line-segments. The transformation represented by Equation (3) can be generalized to the relationship between any point on the left wall of the rectangular room and its corresponding point on the left wall of the Ames room. The transformation between these corresponding points is scaling, so the lines-of-sight from the viewpoint at the origin to the corresponding points coincides with one another. This means that the retinal image of the left wall of the Ames room, seen from the viewpoint (the hole in the viewing wall), is identical to the retinal image of the left wall of the rectangular room seen from the viewpoint. In the same way, the transformation represented by Equation (4) can be generalized to the relationship between any point on the right wall of the rectangular room and its corresponding point on the right wall of the Ames room.

Figure 2. The orthographic images of the Ames room (solid) and of the rectangular illusory room (dotted) from its front, side, and top views. The orthographic images of these two rooms are superimposed on one another so that their viewpoints (black dots) coincide with one another and that the line-of-sight (dashed) from the viewpoint to each vertex of the rectangular room coincides with the line-of-sight to its corresponding vertex of the Ames room.

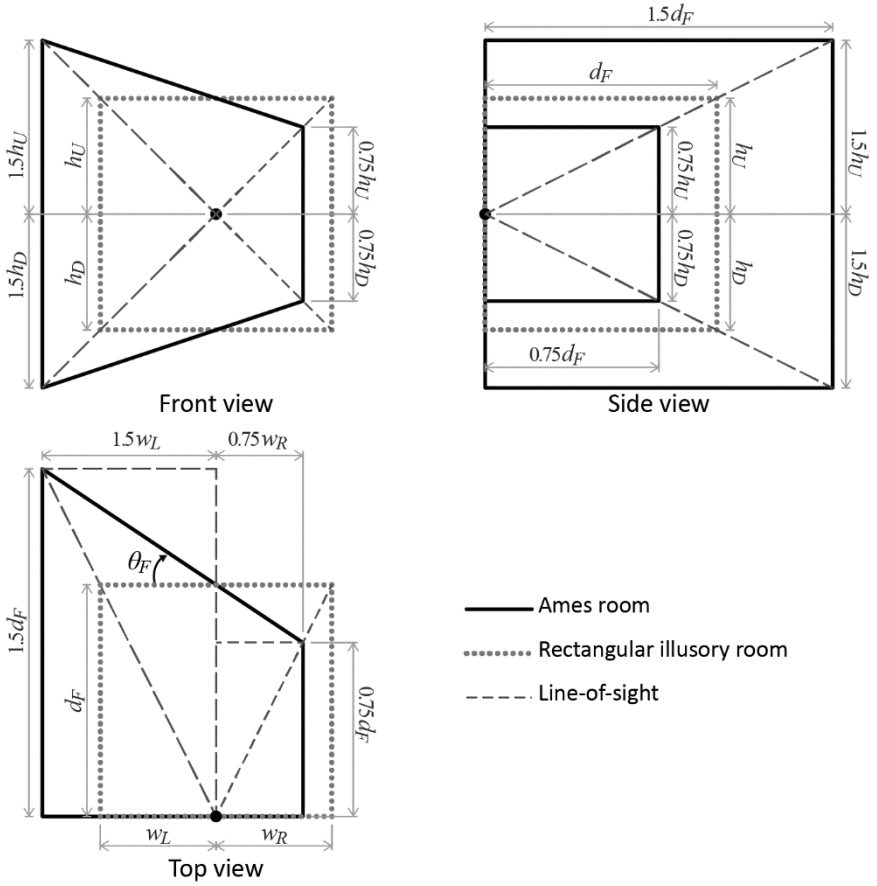

From the top views of the rooms (Figure 2), the orientation θ_F of the facing wall is computed as 33.7° by solving the following equation:

$$\frac{w_L}{d_F} = \frac{w_R}{d_F} = \frac{s_L w_L}{d_F + s_L w_L \tan\theta_F} = \frac{s_R w_R}{d_F - s_R w_R \tan\theta_F}$$

(5)

where $\tan\theta_F = 2/3$. Then, the scaling factors $s_L = 1.5$ and $s_R = 0.75$ can be written as:

$$s_L = \frac{d_F}{d_F + (-w_L)\tan\theta_F}$$

$$s_R = \frac{d_F}{d_F + w_R \tan\theta_F}$$

(6)

These relationships between the four vertices V_{LGF}, V_{LCF}, V_{RGF}, and V_{RCF} in the facing wall of the rectangular room and the four vertices V'_{LGF}, V'_{LCF}, V'_{RGF}, and V'_{RCF} in the facing wall of the Ames room can be generalized to the relationship between any point $V_F = [X_F\ Y_F\ d_F]^t$ on the facing wall of the rectangular room and its corresponding point V'_F on the facing wall of the Ames room as:

$$V'_F = s(X_F)V_F$$

(7)

where the scaling factor $s(X_F)$ depends on the X-coordinate X_F of V_F:

$$s(X) = \frac{d_F}{d_F + X\tan\theta_F}$$

(8)

The plane of the facing wall of the rectangular room is $Z = d_F$ and V_F in this plane is transformed to V'_F in the following plane:

$$Z = -X\tan\theta_F + d_F$$

(9)

This is the plane of the facing wall of the Ames room, so, Equations (7, 8) represent the transformation from the planes of the facing wall of the rectangular room to the plane of the facing wall of the original Ames room. The transformation from V to V' is scaling, so the line-of-sight from the viewpoint at the origin to V_F coincides with the line-of-sight to V'_F. Note that the transformation of Equations (7, 8) also includes the transformations of Equations (3, 4) from the left and right walls of the rectangular room to the left and right walls of the Ames room.

Equations (7, 8) can be further generalized to the relationship between any point $V = [X\ Y\ Z]^t$ in the scene of the rectangular room and its corresponding point $V' = [X'\ Y'\ Z']^t$ in the scene of the Ames room. The transformation of Equations (7, 8) from the rectangular room to the Ames room can be represented by using the homogeneous coordinate system:

$$s\begin{bmatrix} X \\ Y \\ Z \\ U' \end{bmatrix} = \begin{bmatrix} s & 0 & 0 & 0 \\ 0 & s & 0 & 0 \\ 0 & 0 & s & 0 \\ (\tan\theta_F)/d_F & 0 & 0 & 1 \end{bmatrix} \cdot \begin{bmatrix} X \\ Y \\ Z \\ 1 \end{bmatrix} \quad (10)$$

where $V = [X\ Y\ Z]^t$ is a point in the scene of the rectangular room and its corresponding point in the scene of the Ames room is $V' = [X'\ Y'\ Z']^t = s[X\ Y\ Z]^t/U'$. The parameter s is a scaling factor from the rectangular room to the Ames room and it is equal to one for these rooms that are discussed in this section. This parameter can be an arbitrary positive real number and it does not affect the retinal image of the Ames room seen from the viewpoint (the hole in the viewing wall). Equation (10) can be regarded as a 3D-to-3D perspective transformation. The general perspective transformation is:

$$\begin{bmatrix} U^*X^* \\ U^*Y^* \\ U^*Z^* \\ U^* \end{bmatrix} = \begin{bmatrix} m_{11} & m_{12} & m_{13} & m_{14} \\ m_{21} & m_{22} & m_{23} & m_{24} \\ m_{31} & m_{32} & m_{33} & m_{34} \\ m_{41} & m_{42} & m_{43} & m_{44} \end{bmatrix} \cdot \begin{bmatrix} X \\ Y \\ Z \\ 1 \end{bmatrix} \quad (11)$$

where $m_{14} = m_{24} = m_{34} = 0$, the other 13 elements in the 4×4 matrix of Equation (11) are free parameters, and $V^* = [X^*\ Y^*\ Z^*]^t = [U^*X^*\ U^*Y^*\ U^*Z^*]^t/U^*$ is the perspective transformation of V. Note that 3D-to-3D perspective transformations do not form a group. But, the whole set of 3D-to-3D projective transformations form a group and they are a superset of the perspective transformations (see Niall, 1992, 1999 for studies of the relationship between the 3D-to-3D projective transformation and its perception). The general projective transformation can be also represented by Equation (11) but all of the 16 elements of the 4×4 matrix are free parameters for the projective transformation. Note that the planarity of the faces and the straightness of the line-segments of the rectangular room and the Ames room are group invariants of the projective transformation (see Sawada et al., 2015; Appendix A in Sawada & Farshchi, 2022 for discussions of types of invariants). So, any plane in the scene of the rectangular room is transformed to its corresponding plane in the scene of the Ames room. Any plane can be specified by three or more than three points in the plane. Each planar face of the rectangular room can be specified by its four vertices and its corresponding face of the Ames room can be specified by its four vertices that are coplanar to one another and that correspond with the four vertices of the rectangular room. So, any point on the planar face of the rectangular room is transformed to its corresponding point on the planar face of the Ames room. The transformation from V to V' is scaling, so the line-of-sight from the viewpoint at the origin to V coincides with the line-of-sight to V'. This means that a texture on the face of the rectangular room is also transformed to a texture on the corresponding face of the Ames room in such a way the retinal image of the Ames room seen from the viewpoint (the hole in the viewing wall) is identical to the retinal image of the rectangular room seen from the viewpoint.

The parallelism of the line-segments in the rectangular room is not a group invariant of a 3D-to-3D projective transformation. The four line-segments of the rectangular room, which are parallel to the X-axis, are transformed to line-segments of the Ames room that are not parallel to the X-axis or to one another. These four line-segments of the Ames room converge at $[85.32\ 0\ 0]^t$. Note that the parallel line-segments of the rectangular room can be regarded as converging towards one another at infinity. Then, their convergence is also a group invariant of the projective transformation. Under a 3D-to-2D perspective transformation from a 3D scene to an image plane, the straightness and convergence of the line-segments are model-based invariants.

Note that Ittelson (1952; Ittelson & Ames, 1968) also showed two other monocular distorted rooms. One is a "monocular distorted room no. 2" (Ittelson, 1952, p. 41) and this distorted room can be made by rotating the original Ames room, the "monocular distorted room no. 1" around the Z-axis for 90°. The other distorted room is a "full size monocular distorted room" (Ittelson, 1952, pp. 44–45) and this distorted room can be understood by generalizing Equation (10).

A generalized Ames room

Next, consider generalizing the original Ames room so that the following properties of the generalized Ames room can be controlled: (i) the size and aspect-ratio of a rectangular illusory room, (ii) the viewpoint of an observer, and (iii) the amount of distortion of the Ames room from a rectangular room.

The positions of the eight vertices of the original Ames room are characterized by w_L, w_R, h_D, h_U, d_H, and d_F. These variables can be regarded as free parameters of the generalized Ames room that can control (i) the size and aspect-ratio of a rectangular illusory room and (ii) the viewpoint of an observer. The parameters w_L, w_R, and d_F represent the distances of the left, right, and facing walls of the rectangular room from the viewpoint at the origin. The parameter d_H represents the distance of the remaining wall of the rectangular room from the viewpoint. This wall was referred to as the viewing wall when we discussed the original Ames room in the "Monocular distorted room no. 1" section because the viewpoint was on the viewing wall ($d_H = 0$). In the latter part of this study, the wall is referred to as the hind wall because the viewpoint can be distant from and, in front of, the hind wall ($d_H > 0$). The parameters h_D and h_U represent the distances of the floor and the ceiling from the viewpoint. The width, height, and depth of the room are w_L+w_R, h_D+h_U, and d_H+d_F. These parameters should be zero or positive. Otherwise, the viewpoint will be outside of the room.

The orientation of the facing wall of the generalized Ames room is regarded as a free parameter and this parameter controls (iii) the amount of distortion of the Ames room from a rectangular room. The distortion is zero when $\theta_F = 0$.

The orientations of the six faces of the generalized Ames room can be computed as follows once the free parameters of the Ames room are specified. The planes of the left and right walls of the Ames room are $X = -s_L w_L$ and $X = s_R w_R$. The plane of the facing wall is Equation (9) and the plane of the hind wall is:

$$Z = \frac{d_B}{d_F} X \tan\theta_F - d_H \tag{12}$$

The planes of the floor and ceiling of the Ames room are:

$$Y = \frac{-s_R h_D + s_L h_D}{s_R w_R + s_L w_L} X - h_D \tag{13}$$

$$Y = \frac{s_R h_U - s_L h_U}{s_R w_R + s_L w_L} X + h_U \tag{14}$$

Using this formulation, the "full size monocular distorted room" in Ittelson (1952, pp. 44–45) can be specified as: $w_L = w_R = 135.33$ cm (4.44 ft), $h_D = 142.65$ cm (4.68 ft), $h_U = 69.80$ cm (2.29 ft), $d_H = 0$ cm, $d_F =$

323.39 cm (10.61 ft), and $\theta_F = 38.5°$.[2] Note that the "monocular distorted room no. 1" (Ittelson, 1952, pp. 39–43) is mirror-symmetrical about the horizontal plane but the "full size monocular distorted room" is asymmetrical because $h_D \neq h_U$. The rectangular illusory room of the "full size monocular distorted room" is not a cube but a right-angled parallelepiped.

An example of the generalized Ames room is shown in Figure 3. The viewpoint is not on the hind wall of the Ames room but within the Ames room. All the four walls of the Ames room are vertical. The left and right walls of the generalized Ames room are rectangles that have the same aspect-ratio as the left and right walls of the rectangular room. The facing and hind wall, the floor, and the ceiling are trapezoids. They can be either isosceles- or scalene-trapezoids and their shapes can be different from one another.

Figure 3. (A) A generalized Ames room constructed by using the method proposed in this study. The free parameters of the model are set as: $w_L = 14.22$, $w_R = 28.44$, $h_D = 10.66$, $h_U = 32.00$, $d_H = 25.60$, and $d_F = 17.06$, and $\theta_F = 33.7°$. With this parameter setting, the viewpoint (black dot) is within the Ames room. An image of its rectangular illusory room (dotted) is superimposed. The viewing orientation can be arbitrary as far as the viewpoint stays the same. (B) A grid texture for the square faces of the rectangular room and its transformations for the (C) facing wall, (D) floor, (E) ceiling, and (F) hind wall of the generalized Ames room (A). The shapes of the left and right walls of the generalized Ames room are the same as the shapes of the left and right walls of the rectangular room.

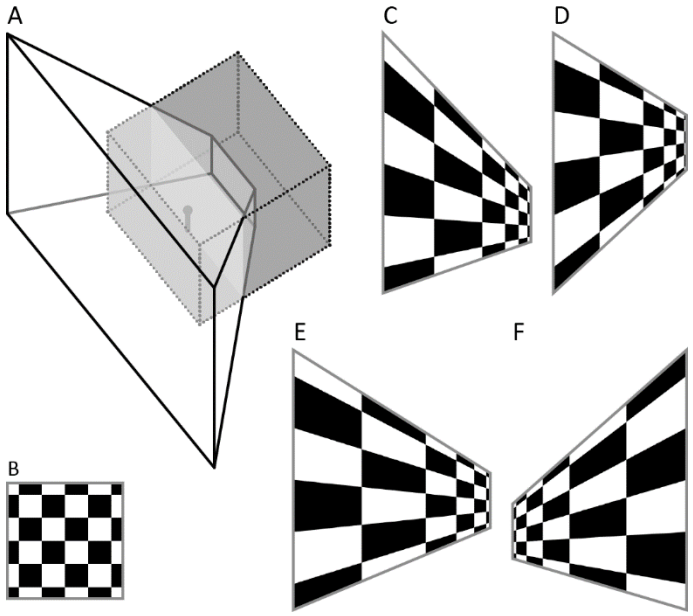

Next, consider generating textures on the faces of the generalized Ames room by transforming textures of the faces of the rectangular illusory room (Figures 3D-H). The textures of the left and right walls

[2] The line-segment between the hind wall and the floor of the "full size monocular distorted room" is computed to be 323.09 cm (10.60 ft) long but the length of this line-segment is specified as 335.28 cm (11.0 ft) in Ittelson (1952, p. 45). We confirmed that the computed length (323.09 cm) is more consistent with an image of the floor in Ittelson (1952, p. 45) than the specified length (335.28 cm) is.

of the Ames room can be generated by scaling the textures of the left and right walls of the rectangular room.

The transformation of a texture from the facing wall of the rectangular room to the facing wall of the Ames room is a 2D-to-2D perspective transformation with the viewpoint at the origin as a center of the projection. To consider this transformation, the 2D xy Cartesian coordinate system is set to each of the two facing walls as follows. The origin of the 2D coordinate system is set at an intersection of the plane of the facing wall with the Z-axis of the 3D coordinate system of the scene. The y-axis of the 2D coordinate system is on the plane of the wall and it is parallel to the Y-axis of the 3D coordinate system. The x-axis of the 2D coordinate system is perpendicular to the y-axis. A point $[x\ y]^t$ on the facing wall of the rectangular room and its perspective transformation $[x'\ y']^t$ to the facing wall of the Ames room are represented as $[x\ y\ z_F]^t$ and $[x'\cos\theta_F\ y'-x'\sin\theta_F+d_F]^t$ using the 3D coordinate system of the scene. The perspective transformation from $[x\ y]^t$ to $[x'\ y']^t$ can be represented by using the homogeneous coordinate system (Figure 3C):

$$\begin{bmatrix} u'x' \\ u'y' \\ u' \end{bmatrix} = \begin{bmatrix} z_F/\cos\theta_F & 0 & 0 \\ 0 & z_F & 0 \\ \tan\theta_F & 0 & z_F \end{bmatrix} \cdot \begin{bmatrix} x \\ y \\ 1 \end{bmatrix} \quad (15)$$

where $[x'\ y']^t = [u'x'\ u'y']^t/u'$. In similar ways, textures of the floor, ceiling, and hind wall of the rectangular room can be transformed for the floor, ceiling, and hind wall of the Ames room as:

$$\begin{bmatrix} u'x' \\ u'y' \\ u' \end{bmatrix} = \begin{bmatrix} q/\cos\theta_Q & 0 & 0 \\ 0 & q & 0 \\ -\tan\theta_Q & 0 & q \end{bmatrix} \cdot \begin{bmatrix} x \\ y \\ 1 \end{bmatrix} \quad (16)$$

For the floor (Figure 3D), $q = -h_D$ and:

$$\theta_Q = \tan^{-1}\left(\frac{-s_R h_D + s_L h_D}{s_R w_R + s_L w_L}\right) \quad (17)$$

For the ceiling (Figure 3E), $q = h_U$ and:

$$\theta_Q = \tan^{-1}\left(\frac{s_R h_U - s_L h_U}{s_R w_R + s_L w_L}\right) \quad (18)$$

For the hind wall (Figure 3F), $q = d_H$ and:

$$\theta_Q = \tan^{-1}\left(\frac{d_H}{d_F}\tan\theta_F\right) \quad (19)$$

The model for constructing a shape of a generalized Ames room is implemented as a C# script of Unity 3D (ver. 2021.3.18f1, https://unity.com/) and the model for transforming textures of a rectangular illusory

room to textures of the generalized Ames room is implemented as a Python script using OpenCV (https://github.com/TadamasaSawada/AmesRoom). These implementations allow us to construct the Ames room in a VR space and to control the Ames room systematically and quantitatively.

An Ames scene

In this section, we discuss the further generalization of the transformation that was discussed in the last two sections. Equation (10), which distorts a rectangular illusory room to an Ames room, can be generalized as:

$$\begin{bmatrix} X \\ Y \\ Y \\ U'' \end{bmatrix} = \begin{bmatrix} 1 & 0 & 0 & 0 \\ 0 & 1 & 0 & 0 \\ 0 & 0 & 1 & 0 \\ m_{41} & m_{42} & m_{43} & m_{44} \end{bmatrix} \cdot \begin{bmatrix} X \\ Y \\ Z \\ 1 \end{bmatrix} \tag{20}$$

where m_{41}, m_{42}, m_{43}, and m_{44} are free parameters, $V = [X\ Y\ Z]^t$ is a point in the scene of the rectangular room, and its transformation is $V'' = [X''\ Y''\ Z'']^t = [X\ Y\ Z]^t/U''$. The lines-of-sight from the viewpoint at the origin to the corresponding points V and V'' coincides with one another. The parameters m_{41}, m_{42}, and m_{43} characterizes the degrees of the distortion along the X-, Y-, and Z-axis and the parameter m_{44} characterizes the scaling.

The transformation of Equation (20) is still a 3D-to-3D perspective transformation, which is a subset of 3D-to-3D projective transformations (Equations 11). Any plane and any line-segment within the scene of the rectangular room is transformed to its corresponding plane and line-segment within the scene of the Ames room. Any set of parallel or converging line-segments within the scene of the rectangular room is transformed to its corresponding set of parallel or converging line-segments. These are obtained because the planarity of the face, the straightness of the line-segment, and the convergence of the line-segments of the rectangular room and the Ames room are group invariants of the projective transformation (see Sawada et al., 2015; Appendix A in Sawada & Farshchi, 2022).

Note that the transformation represented by Equation (20) can be applied not only to a rectangular room but also an arbitrary 3D scene. The retinal image of the transformed 3D scene seen from the origin is identical to the retinal image of the initial 3D scene seen from the origin before the transformation. There are the same group invariants of the projective transformation between the initial and transformed scene as between the rectangular and Ames rooms. The transformation applied to a pentagonal cylinder is shown in Figure 4A.

Equation (20) can also represent a transformation, including a depth-reversal. Consider an observer seeing the interior of a rectangular hollow cylinder in such a way that the line-of-sight of the observer coincides with the axis of the cylinder. The cylinder has one open section and is infinitely long from the open section to the other direction. The observer sees the cylinder's interior through this open section. The four lines of the cylinder that are parallel to the axis of the cylinder are projected to four line-segments in the retinal image of the observer that emanate from their vanishing point. This cylinder can be transformed by Equation (20) to a rectangular cone whose apex is pointing towards the observer, for example, when $m_{41} = m_{42} = 0$, $m_{43} = 1$ and $m_{44} = -0.5$ (Figure 4B). The four ridges of the cone correspond to the four line-segments of the cylinder. The retinal image of the cone's apex coincides with the vanishing point. This transformation can be relevant to the "reverspective" (see Papathomas & Hughes, 2019), which is another geometrical illusion.

Figure 4. (A) A room that has the shape of a pentagonal cylinder (dotted) and its distorted shape (solid). The retinal images of these rooms are identical to one another when they are seen from a specific viewpoint inside the room (black dot). The pentagonal shape is transformed to the distorted shape by using Equation (20): $m_{41} = 0.039$, $m_{42} = m_{43} = 0$, and $m_{44} = 1$. This transformation is equivalent to the transformation for the distorted room in Figure 3A: $m_{41} = \tan(33.7°)/17.06 = 0.039$. (B) A rectangular hollow cylinder (dotted) and a rectangular cone (solid) that is generated by distorting the cylinder. The retinal image of the interior space of the cylinder that is seen from a specific viewpoint (black dot) is identical to the retinal image of the cone that is seen from above the cone. The axis of the cone coincides with the axis of the cylinder (dashed) and the viewpoint is on the axis. The cylinder is transformed to the cone by using Equation (20): $m_{41} = m_{42} = 0$, $m_{43} = 1$, and $m_{44} = -0.5$.

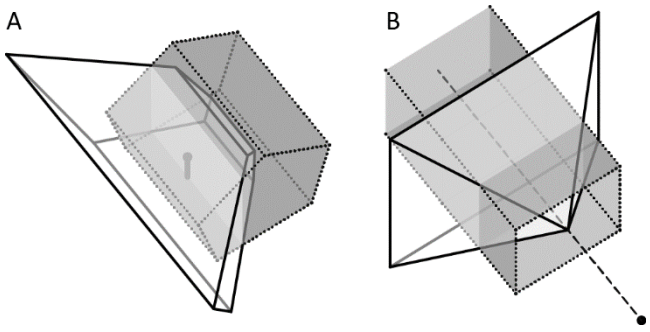

Now, consider transforming a texture from a plane in the initial scene to its corresponding plane in the transformed scene. This transformation is represented as a 2D-to-2D perspective transformation. First, the 2D *xy* Cartesian coordinate system is set to the initial plane. The position of the origin and the orientation of the x-axis are arbitrary in the initial plane. The orientation of the y-axis is perpendicular to the x-axis in the initial plane. The position of the origin of the initial plane is represented as a 3D column vector V_O in the initial 3D scene. The orientations of the x- and y-axes of the initial plane are represented as unit 3D column vectors V_X and V_Y in the initial 3D scene where $\|V_X\| = \|V_Y\| = 1$ and $V_X \cdot V_Y = 0$. Any point in the initial plane can be represented as $V_{\alpha\beta} = V_O + \alpha V_X + \beta V_Y$ where α and β are the 2D x- and y-coordinates $[\alpha\ \beta]^t$ of the point $V_{\alpha\beta}$ in the initial plane.

Next, the 2D *xy* Cartesian coordinate system is set to the transformed plane so that the origin and the x-axis in the transformed plane is the perspective transformation of the origin and the x-ais in the initial plane by using Equation (20). The y-axis in the transformed plane is perpendicular to the x-axis in the transformed plane. This y-axis is usually not the perspective transformation of the y-axis in the initial plane. The position of the origin of the transformed plane is represented as:

$$V''_O = \frac{V_O}{U''_O} \tag{21}$$

where $U''_0 = [m_{41} \quad m_{42} \quad m_{43}] \cdot V_O + m_{44}$. The perspective transformation of $V_{\alpha\beta}$ in the initial plane is:

$$V''_{\alpha\beta} = \frac{V_O + \alpha V_X + \beta V_Y}{U''_O + \alpha \widetilde{U}_X + \beta \widetilde{U}_Y}$$

(22)

where $\widetilde{U}_X = [m_{41} \quad m_{42} \quad m_{43}] \cdot V_X$ and $\widetilde{U}_Y = [m_{41} \quad m_{42} \quad m_{43}] \cdot V_Y$. The relative position of $V''_{\alpha\beta}$ to V''_O can be represented as the sum of two vectors V''_X and V''_Y:

$$V''_{\alpha\beta} - V''_O = \frac{\alpha}{U''_O + \alpha\widetilde{U}_X + \beta\widetilde{U}_Y} V''_X + \frac{\beta}{U''_O + \alpha\widetilde{U}_X + \beta\widetilde{U}_Y} V''_Y$$

(23)

where:

$$\begin{cases} V''_X = V_X - \dfrac{\widetilde{U}_X}{U''_O} V_O \\ V''_Y = V_Y - \dfrac{\widetilde{U}_Y}{U''_O} V_O \end{cases}$$

These vectors V''_X and V''_Y are normalized to unit vectors $\hat{V}''_X = V''_X / \|V''_X\|$ and $\hat{V}''_Y = V''_Y / \|V''_Y\|$ where $\left\|\hat{V}''_X\right\| = 1$ and $\left\|\hat{V}''_Y\right\| = 1$. The vectors $\hat{V}''_X$ and $\hat{V}''_Y$ represent the orientations of two lines in the transformed plane that are the perspective transformations of the x- and y-axes of the 2D xy coordinate system in the initial plane. The vectors $\hat{V}''_X$ and $\hat{V}''_Y$ are usually not perpendicular to one another. The x-axis in the transformed plane is set to be parallel to $\hat{V}''_X$. The orientation of the y-axis in the transformed plane is represented by a vector $\left(\hat{V}''_Y + k\hat{V}''_X\right)$ where $k = -\hat{V}''^{t}_X \cdot \hat{V}''_Y$ and $\hat{V}''^{t}_X \cdot \left(\hat{V}''_Y + k\hat{V}''_X\right) = 0$. Then, Equation (23) can be re-written as:

$$V''_{\alpha\beta} - V''_O = \frac{\alpha\|V''_X\| - k\beta\|V''_Y\|}{U''_O + \alpha\widetilde{U}_X + \beta\widetilde{U}_Y} \hat{V}''_X + \frac{\beta\|V''_Y\|}{U''_O + \alpha\widetilde{U}_X + \beta\widetilde{U}_Y} \left(\hat{V}''_Y + k\hat{V}''_X\right)$$

(24)

From Equation (24), the 2D x- and y-coordinates $[\alpha'' \beta'']^t$ of the point $V''_{\alpha\beta}$ in the transformed plane is:

$$\begin{cases} \alpha'' = \dfrac{\alpha\|V''_X\| - k\beta\|V''_Y\|}{U''_O + \alpha\widetilde{U}_X + \beta\widetilde{U}_Y} \\ \beta'' = \dfrac{\beta\|V''_Y\|\sqrt{1-k^2}}{U''_O + \alpha\widetilde{U}_X + \beta\widetilde{U}_Y} \end{cases}$$

(25)

where $\sqrt{1-k^2} = \left\|\hat{V}''_Y + k\hat{V}''_X\right\|$. From Equation (25), the 2D-to-2D perspective transformation from the initial plane to the transformed plane can be written as:

$$\begin{bmatrix} u''\alpha'' \\ u''\beta'' \\ u'' \end{bmatrix} = \begin{bmatrix} \|V''_X\| & -k\|V''_Y\| & 0 \\ 0 & \|V''_Y\|\sqrt{1-k^2} & 0 \\ \widetilde{U}_X & \widetilde{U}_Y & U''_O \end{bmatrix} \cdot \begin{bmatrix} \alpha \\ \beta \\ 1 \end{bmatrix}$$

(26)

Discussion

The geometrical properties of an Ames room were analyzed in this study and the generalization of the Ames room was discussed. The first generalization was proposed as a computational model that consists of two components: (i) constructing a 3D shape of an Ames room and (ii) generating textures of the faces of the Ames room by transforming textures of the faces of the rectangular room. These components of the model are implemented as a C# script of Unity 3D and a Python script using OpenCV (https://github.com/TadamasaSawada/AmesRoom) so that the Ames room can be constructed in a VR space. This implementation makes the illusion portable and it allows us to study this illusion without constructing any real Ames rooms while systematically controlling many features of our Ames room. It also allows us to design an Ames room depending on available size of a real space to physically construct the Ames room in the real space.

The distortion from the rectangular room to the Ames room is formulated as a 3D-to-3D perspective transformation. This formulation allows us to apply the same distortion to an arbitrary 3D scene as to a rectangular illusory room for the Ames room. This transformation can be regarded as a member of a subset of 3D-to-3D perspective transformations. Any perspective transformation in this subset distorts the 3D scene in such a way that the retinal image of the distorted scene, when seen from a specific viewpoint, is identical to the retinal image of the initial scene, when seen from a specific viewpoint. Note that the "reverspective" (see Papathomas & Hughes, 2019), which is another geometrical illusion, can be also characterized by this transformation.

These generalizations allow us to control the conditions of an Ames room quantitatively when we study this illusion. For example, the visual angle and the viewing distance of the facing wall can be systematically controlled for studying the effects of binocular cues on the Ames room illusion. These effects have been examined in several studies (Dorward & Day, 1997; Gehringer & Engel, 1986; Ittelson, 1960, pp. 160-163; Pilewski & Martin, 1991, see also Gibson, 1979, p. 168; Runeson, 1988) and these studies showed that the illusion is still effective but it is weaker when these Ames rooms are seen binocularly. Gehringer and Engel (1986) used the "monocular distorted room no. 1" (Ittelson, 1952, pp. 39–43) and Dorward and Day (1997) used the one-tenth scale version of the "full size monocular distorted room" (Ittelson, 1952, pp. 44–45).[3] The viewing distances to the facing walls (d_F in the proposed model of this study when $s = 1$) are 108.36 cm in Gehringer and Engel (1986) and 32.34 cm in Dorward and Day (1997). These are short enough for the binocular cues to operate. The visual angles of the facing walls are 53.1° × 53.1° in Gehringer and Engel (1986) and 45.42° × 35.98° in Dorward and Day (1997). These visual angles may have been too large for the binocular disparity cue to operate. Note that the interiors of these distorted rooms are uniformly colored. So, the edges of the facing walls could be the primary visual features used to perceive the orientations of the facing walls from the binocular disparity cue. The effects of the binocular cues can become larger if the illusion is tested with a smaller visual angle of the facing wall or if the facing wall has with a texture pattern. Another example is the height of the viewpoint from the floor (h_D in the proposed model of this study). The position of the viewpoint relative to a plane is an important factor for perceiving positions of objects on the plane (Kwon et al., 2016; Ooi & He, 2007; Meng & Sedgwick, 2001; Sedgwick, 2021). Using the computational implementation of the model, an Ames room can be constructed in a virtual space of 3D computer graphics software. Once this is done, many other parameters, such as texture (e.g. random noise pattern, https://youtu.be/CfF_rLsPEt8?t=37), can be also controlled by using software functions.

[3] Dorward and Day (1997) reported that they used the one-tenth scale version of the "Ames No 1 room" but the dimensions of their distorted room and Figure 1 in Dorward and Day (1997) indicate that they actually used the one-tenth version of the "full size monocular distorted room" (Ittelson, 1952, pp. 44–45).

The computational model of the generalized Ames room also allows us to systematically control a psychophysical experiment that tests the Ames room illusion. Note that the Ames rooms that were used in the past studies were distorted to a fixed degree in such a way that the left side of the facing wall was further than the right side of the facing wall (see Figures 1 and 3). The degree of the distortion and its direction should be variable and should be randomized across trials to minimize the response biases of the participants. These variables can be controlled by our model.

Acknowledgements

This article is an output of a research project implemented as part of the Basic Research Program at the National Research University Higher School of Economics (HSE University) in 2024.

References

Behrens, R. R. (1987). The Life and Unusual Ideas of Adelbert Ames, Jr. Leonardo, 20(3), 273–279. https://doi.org/10.2307/1578173

Brecher, K., & Puno, R. (2010). Project LITE: Ames room demonstration. Boston University. https://www.bu.edu/lite/inkjet-science/index.html

Cowan, T. M. (1974). The theory of braids and the analysis of impossible figures. Journal of Mathematical Psychology, 11(3), 190–212. https://doi.org/10.1016/0022-2496(74)90018-2

Cowan, T. M. (1977a). Organizing the properties of impossible figures. Perception, 6(1), 41–56. https://doi.org/10.1068/p060041

Cowan, T. M. (1977b). Supplementary report: Braids, side segments, and impossible figures. Journal of Mathematical Psychology. Journal of Mathematical Psychology, 16(3), 254–260. https://doi.org/10.1016/0022-2496(77)90055-4

Cowan, T. M. (1982). Turning a Penrose triangle inside out. Journal of Mathematical Psychology, 26(3), 252–262. https://doi.org/10.1016/0022-2496(82)90004-9

Day, R. H. (1993). The Ames room from another viewpoint. Perception, 22(9), 1007–1011. https://doi.org/10.1068/p221007

Dorward, F. M. C., & Day, R. H. (1997). Loss of 3-D shape constancy in interior spaces: The basis of the Ames-room illusion. Perception, 26(6), 707–718. https://doi.org/10.1068/p260707

Dvoeglazova, M., Koshmanova, E., & Sawada, T. (2021). Visual sensitivity to parallel configurations of contours compared with sensitivity to other configurations. Vision Research, 188, 149–161. https://doi.org/10.1016/j.visres.2021.07.006

Dvoeglazova, M., & Sawada, T. (2024). A role of rectangularity in perceiving a 3D shape of an object. *Vision Research, 221*, Article 102841. https://doi.org/10.1016/j.visres.2024.108433.

Gehringer, W. L., & Engel, E. (1986). Effect of ecological viewing conditions on the Ames' distorted room illusion. Journal of Experimental Psychology: Human Perception and Performance, 12(2), 181–185. https://doi.org/10.1037/0096-1523.12.2.181

Gibson, J. J. (1979). The ecological approach to visual perception. New York, NY: Psychology Press.

Gogel, W. C., & Mershon, D. H. (1968). The perception of size in a distorted room. Perception & Psychophysics, 4(1), 26–28. https://doi.org/10.3758/BF03210442

Goldstein, E. B. (2007). Sensation and perception (8th ed.). Wadsworth, Cengage Learning.

Gregory, R. L. (1966). Eye and brain: The psychology of seeing. McGraw-Hill.

Ittelson, W. H. (1952). The Ames demonstrations in perception: A guide to their construction and use. Princeton University Press.

Ittelson, W. H. (1960). Visual space perception. Springer.

Ittelson, W. H., & Ames, A. Jr. (1968). *The Ames demonstrations in perception - together with an interpretative manual – with a new introduction*. Hafner Publishing Company.

JoVE Science Education Database (2023). Sensation and Perception: The Ames room. JoVE. https://app.jove.com/v/10292/the-ames-room

Kerr, N. L. (1998). HARKing: Hypothesizing after the results are known. Personality and social psychology review, 2(3), 196-217. https://doi.org/10.1207/s15327957pspr0203_4

Koshmanova, E., Dvoeglazova, M., Myrov, V., Gorina, E., Vodorezova, K., Gorbunova, E., & Sawada, T. (in-press). The Ames room and the misunderstood versions and depictions. Perception. (PsyArXiv. https://doi.org/10.31234/osf.io/xgcvh)

Kwon, T., Li, Y., Sawada, T., & Pizlo, Z. (2016). Gestalt-like constraints produce veridical (Euclidean) percepts of 3D indoor scenes. Vision Research, 126, 264–277. https://doi.org/10.1016/j.visres.2015.09.011

Li, Y., Sawada, T., Latecki, L.M., Steinman, R.M., & Pizlo, Z. (2012). A tutorial explaining a machine vision model that emulates human performance when it recovers natural 3D scenes from 2D images. *Journal of Mathematical Psychology, 56*(4), 217–231. https://doi.org/10.1016/j.jmp.2012.07.001

Meng, J. C., & Sedgwick, H. A. (2001). Distance perception mediated through nested contact relations among surfaces. Perception & Psychophysics, 63(1), 1–15. https://doi.org/10.3758/bf03200497

Minkov V., & Sawada T. (2021). Theoretical treatment of limitations inherent in simple 3D stimuli: Triangles and the P3P problem. *Vision, 5*(1), 10. https://doi.org/10.3390/vision5010010

Mischenko, E., Negishi, I., Gorbunova, E. S., & Sawada, T. (2020). Examining the role of familiarity in the perception of depth. *Vision, 4*(2), Article 21. https://doi.org/10.3390/vision4020021

Niall, K. K. (1992). Projective invariance and the kinetic depth effect. *Acta Psychologica, 81*(2), 127–168. https://doi.org/10.1016/0001-6918(92)90003-V

Niall, K. K. (1999). Estimates of shape by eye, or, The little invariant that could. *Acta Psychologica, 100*(3), 291–320. https://doi.org/10.1016/S0001-6918(98)00042-0

Ooi, T. L., & He, Z. J. (2007). A distance judgment function based on space perception mechanisms: Revisiting Gilinsky's (1951) equation. Psychological Review, 114(2), 441–454. https://doi.org/10.1037/0033-295X.114.2.441

Papathomas, T. V., & Hughes, P. (2019). Hughes's reverspectives: Radical uses of linear perspective on non-coplanar surfaces. *Vision, 3*(4), 63. https://doi.org/10.3390/vision3040063

Pilewski, J. L., & Martin, B. A. (1991). Effects of monocular versus binocular viewing in the Ames Distorted-Room illusion. Perceptual and motor skills, 72(1), 306–306. https://doi.org/10.2466/pms.1991.72.1.306

Pizlo, Z. & Salach-Golyska, M. (1994) Is vision metric? Comment on Lappin and Love. Perception and Psychophysics, 55, 230–234. https://doi.org/10.3758/bf03211670

Pizlo, Z., Li, Y., Sawada, T., & Steinman, R. M. (2014). Making a machine that sees like us. Oxford University Press. https://doi.org/10.1093/ACPROF:OSO/9780199922543.001.0001

Rogers, B. (2022). When is an illusion not an illusion? An alternative view of the illusion concept. Frontiers in Human Neuroscience, 17, Article 957740. https://doi.org/10.3389/fnhum.2022.957740

Rossing, T. D., & Chiaverina, C. J. (2019). Light science. Springer.

563 Runeson, S. (1988). The distorted room illusion, equivalent configurations, and the specificity of static optic
564 arrays. Journal of Experimental Psychology: Human Perception and Performance, 14(2), 295–304.
565 https://doi.org/10.1037/0096-1523.14.2.295

566 Sawada, T., & Dvoeglazova, M. (2023). Commentary: Rectangularity is stronger than symmetry in interpreting
567 2D pictures as 3D objects. Frontiers in Human Neuroscience, 17, Article 1138287.
568 https://doi.org/10.3389/fnhum.2023.1138287

569 Sawada, T., & Farshchi, M. (2022). Visual detection of 3D mirror-symmetry and 3D rotational-symmetry.
570 Visual Cognition, 30(8), 546–563. https://doi.org/10.1080/13506285.2022.2139314

571 Sawada, T., Li, Y., & Pizlo, Z. (2011). Any pair of 2D curves is consistent with a 3D symmetric interpretation.
572 *Symmetry*, 3(2), 365–388. https://doi.org/10.3390/sym3020365

573 Sawada, T., Li, Y., & Pizlo, Z. (2014). Detecting 3-D mirror symmetry in a 2-D camera image for 3-D shape
574 recovery. *Proceedings of the IEEE*, 102(10), 1588–1606.
575 http://dx.doi.org/10.1109/JPROC.2014.2344001

576 Sawada, T., Li, Y., & Pizlo, Z. (2015). Shape perception. In J. Busemeyer, J. Townsend, Z. J. Wang, & A. Eidels
577 (Eds.), Oxford Handbook of Computational and Mathematical Psychology (pp. 255–276). Oxford
578 University Press.

579 Sawada, T., & Pizlo, Z. (2022). Testing a formal theory of perception is not easy: Comments on Yu, Todd &
580 Petrov (2021) and Yu, Petrov & Todd (2021). Journal of Vision, 22(4):15, 1–4.
581 https://doi.org/10.1167/jov.22.4.15

582 Sawada, T., & Volk, D. (2024). An accidental image feature that appears but not disappears. Journal of
583 Mathematical Psychology, 119, Article 102841. https://doi.org/10.1016/j.jmp.2024.102841

584 Sedgwick, H. A. (2021). J. J. Gibson's "ground theory of space perception". i-Perception, 12(3), Article
585 20416695211021111. https://doi.org/10.1177/2041669521102111

586 Simmons, J. P., Nelson, L. D., & Simonsohn, U. (2011). False-positive psychology: Undisclosed flexibility in
587 data collection and analysis allows presenting anything as significant. Psychological science, 22(11),
588 1359–1366. https://doi.org/10.1177/0956797611417632

589 Stewart, V. M. (1974). A cross-cultural test of the "carpentered world" hypothesis using the Ames distorted
590 room illusion. International Journal of Psychology, 9(2), 79–89.
591 https://doi.org/10.1080/00207597408247094

592 Sugihara, K. (1986). Machine Interpretation of Line Drawings. MIT Press.

593 Sugihara, K. (1997). Three-dimensional realization of anomalous pictures—An application of picture
594 interpretation theory to toy design. Pattern Recognition, 30(7), 1061–1067.
595 https://doi.org/10.1016/S0031-3203(96)00138-0

596 Sugihara, K. (2005). A characterization of a class of anomalous solids. Interdisciplinary Information Sciences,
597 11(2), 149–156. https://doi.org/10.4036/iis.2005.149

598 Sugihara, K. (2014a). Design of solids for antigravity motion illusion. Computational Geometry, 47(6), 675–
599 682. https://doi.org/10.1016/j.comgeo.2013.12.007

600 Sugihara, K. (2014b). Right-angle preference in impossible objects and impossible motions. In Proceedings of
601 Bridges 2014: Mathematics, Music, Art, Architecture, Culture (pp. 449–452). Tessellations Publishing.

602 Tyler, C. W. (2022). The nature of illusions: A new synthesis based on verifiability. Frontiers in Human
603 Neuroscience, 16, Article 875829. https://doi.org/10.3389/fnhum.2022.875829

Wang, S., Sanches de Oliveira, G., Djebbara, Z. & Gramann, K. (2022). The embodiment of architectural experience: A methodological perspective on neuro-architecture. Frontiers in Human Neuroscience, 16, Article 833528. https://doi.org/10.3389/fnhum.2022.833528

Wickelgren, I. (2012, October 9). Instant egghead - what is the Ames illusion? Scientific American. https://www.scientificamerican.com/video/instant-egghead-what-is-the-ames2012-10-09/

Williford, K., Bennequin, D., & Rudrauf, D. (2022). Pre-reflective self-consciousness & projective geometry. Review of Philosophy and Psychology, 13(2), 365–396. https://doi.org/10.1007/s13164-022-00638-w

Author contributions statement

TS contributed to the conception. ESG and TS contributed to the supervision. VM and TS contributed to the formulation of the model proposed in this study. VM, EG, KV, and TS contributed to the computational implementation of the model. MD and EK contributed to the review of the past relevant studies. TS wrote the first draft of the manuscript. All the authors reviewed the manuscript and approved the final version of the manuscript for submission.

Accession codes

The scripts of the model proposed in this study can be found in https://github.com/TadamasaSawada/AmesRoom.